JOURNAL OF BACTERIOLOGY, Feb. 1985, p. 750–757
0021-9193/85/020750-08$02.00/0

Vol. 161, No. 2

Three-Dimensional Architecture of the Cell Sheath and Septa of *Methanospirillum hungatei*

PETER J. SHAW,[1]* GRAHAM J. HILLS,[1] JUDITH A. HENWOOD,[1] JANE E. HARRIS,[2] AND DAVID B. ARCHER[2]

John Innes Institute, Norwich NR4 7UH,[1] and Food Research Institute, Norwich NR4 7UA,[2] United Kingdom

Received 18 May 1984/Accepted 25 October 1984

The methanogenic bacterium *Methanospirillum hungatei* exists as filaments which have a very unusual cell wall architecture, comprising a long cylindrical sheath within which there may be many individual cells arranged in a line. The sheath has a two-dimensional crystalline structure, and the cells are separated within the tube by septa which also have a crystalline structure. We have used computer image processing of tilted-view electron micrographs to analyze the structure in negative stains of both of these components in three dimensions. The repeating unit of the sheath consists of four approximately spherical domains ca. 2.5 nm in diameter arranged in a row. Based on observations of the type of lattice imperfections that occur, we suggest that each of the domains represents a separate polypeptide subunit and that the subunits are incorporated into the wall one by one. The septa are circular plates of remarkably constant size. They are normally found as double layers. They are hexagonally symmetrical and consist of trimerically associated subunits which interact about dimer axes to form an open network containing large pores ca. 15 nm in diameter.

Many procaryotic organisms and some simpler eucaryotic organisms have a cell envelope, the outer layer of which consists of a crystalline protein array. Such a layer has been observed for a number of bacteria and has been termed the S-layer (17). Crystalline cell wall layers have also been observed in cyanobacteria and in some green algae, notably the order Volvocales. In the latter organisms, the hydroxyproline-containing glycoprotein subunits of the crystalline layer show marked resemblances to the glycoproteins of higher plant primary cell walls and have been used as model systems for studying the structure, interactions, and assembly of this class of glycoproteins (12, 13, 16).

In the simplest cases, for example, the thermoacidophilic bacterium *Sulfolobus acidocaldarius*, the crystalline layer is virtually the only structural extracellular material and is probably directly attached to the cell membrane (5). In those gram-positive bacteria possessing an S-layer, there is a peptidoglycan layer between the cell membrane and the crystalline layer, whereas in gram-negative bacteria, the S-layer, if present, is attached to the outer face of the outer membrane (17).

The methanogens and certain extremely thermoacidophilic and halophilic bacteria are members of the archaebacteria, which are only distantly related to both the eubacteria and eucaryotes (21). Crystalline cell wall layers have been reported for several methanogenic bacteria (17), but none have been examined previously in any detail. Among the other archaebacteria, several halobacteria have been shown to have crystalline cell wall layers, and the crystalline layer of *S. acidocaldarius* has been analyzed by electron microscopy and three-dimensional image reconstruction (5).

Methanospirillum hungatei is a methanogenic bacterium which possesses an extremely unusual and possibly unique architecture (22). Single cells which possess a crystalline outer sheath are occasionally found, but more usually cell division within the outer sheath produces long filaments which may contain many cells (22). These filaments, which are only slowly motile, are wound into helices. The crystalline outer sheath is composed of protein, and there is an amorphous inner layer which surrounds the individual cells within the outer sheath. Carbohydrate is associated with the sheaths, but it is not known whether any of it is covalently linked to the protein (19). Within the sheath, the cells are separated by spacer elements which have been termed septa. The septa generally occur in pairs separated by a gap region containing amorphous material (22). The filaments have also been reported to contain an end structure which has the appearance of a square plate in which a regular structure is visible (22).

Treatment of the *M. hungatei* filaments with dithiothreitol releases spheroplasts—single cells which appear to retain at least part of the inner wall covering—and leaves behind empty cell sheaths (18). The spherical shape of these single cells shows the flexibility of the inner layer; the filament shape must be determined primarily by the cell sheath and its associated components. Attachment of the inner wall and cell spacers to the outer sheath must presumably involve disulfide bonds.

Although the general morphology and ultrastructure of the cells have been studied, mainly by electron microscopy of thin sections, no detailed structural study has been made of any of the extracellular components. We have investigated the three-dimensional architecture of the cell wall components by electron microscopy and image processing, both for comparison with other extracellular surface layers and for elucidation at the molecular level of the unusual architecture of this organism.

MATERIALS AND METHODS

Culture procedure. *M. hungatei* JF1 (DSM 864) was grown in M3 medium prepared by the anaerobic techniques of Hungate (9). M3 medium contained the following (grams per liter): yeast extract (5), sodium formate (2), sodium acetate (2), sodium chloride (0.9), ammonium sulfate (0.9), potassium dihydrogen phosphate (0.45), dipotassium hydrogen phosphate (0.9), calcium chloride ($CaCl_2 \cdot 6H_2O$) (0.2), magnesium sulfate ($MgSO_4 \cdot 7H_2O$) (0.2), ferrous sulfate ($FeSO_4 \cdot 7H_2O$) (0.01), resazurin (0.001), and the trace mineral solution (10 ml/liter) described by Archer and King (1).

* Corresponding author.

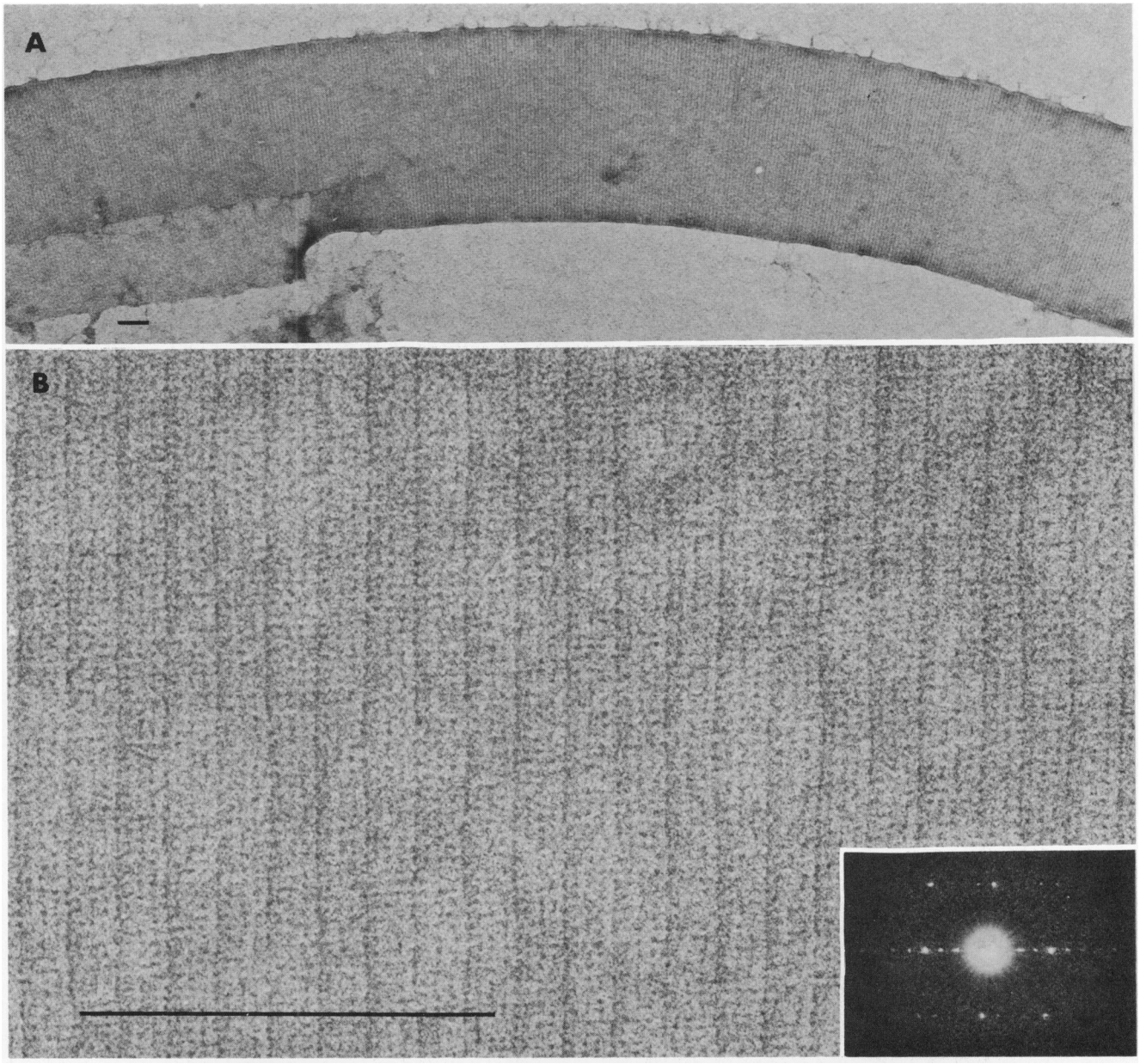

FIG. 1. Cell sheath of *M. hungatei*. (A) Low-magnification view showing the curved conformation of the sheath. A portion of the sheath has split open, showing a single layer. Bar, 100 nm. (B) High-magnification view of an area of a single layer. Bar, 100 nm. The inset is an optical diffraction pattern of the sheath.

The medium was prepared in 400-ml amounts in 1-liter Duran bottles (Schott, Mainz, West Germany) modified to incorporate a glass tube with a butyl rubber septum similar to that described by Balch et al. (2). After the medium was boiled and cooled under an N_2-CO_2 (80:20) atmosphere, sodium carbonate (Na_2CO_3) (2 g/liter) was added, and the pH was adjusted to 6.8. The medium was reduced with cysteine-hydrochloride (0.4 g/liter) and sodium sulfide ($Na_2S \cdot 9H_2O$) (0.4 g/liter) before being autoclaved.

The medium was inoculated in an aerobic cabinet (model 1024; Forma Scientific, Marietta, Ohio) with a 2% (vol/vol) log-phase culture in M3 medium. The headspace gas was replaced with H_2-CO_2 (80:20) at 2 bars pressure. Cultures were incubated at 37°C, left stationary for 24 h, and then shaken. The headspace gas was replenished daily.

Growth was monitored by measuring methane production (1), and the cells were harvested without anaerobic precautions at the late log phase by centrifugation at 15,000 × *g* for 30 min. The pellet of cells was stored at 4°C in the presence of 0.2% sodium azide.

Electron microscopy. Cell sheaths were disrupted with glass Ballotini beads in a Mickle shaker, followed by several cycles of centrifugation and suspension in water. This procedure emptied most of the sheaths.

Cells for sectioning were fixed in 2% glutaraldehyde (buffered to pH 7.2 with 0.05 M cacodylate), postfixed in osmium tetroxide, dehydrated, embedded in LR resin (London Resin Co., Basingstoke, Hants, United Kingdom), and stained with uranyl acetate and lead citrate after being sectioned.

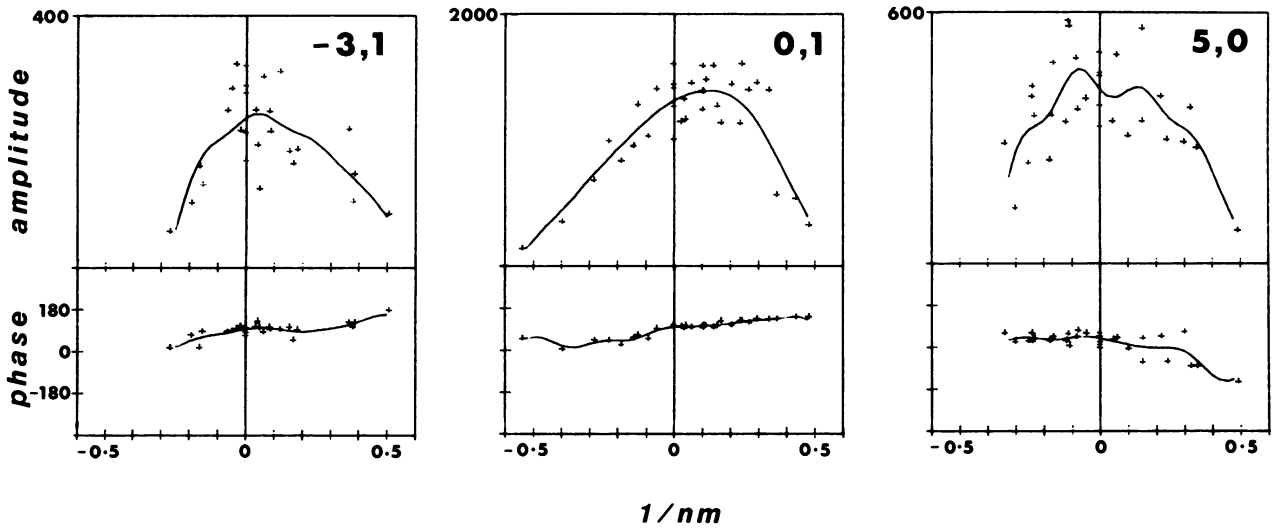

FIG. 2. Selection of z* lattice lines for the sheath structure. For each line, amplitude and phase datum points are plotted as a function of z* (the reciprocal cell dimension normal to a* and b*), together with the smooth curves derived from the points by a constrained least-squares fit procedure (Shaw, in press). The selection was made so as to show representative samples, including both axial and nonaxial lines and lines both strong and weak in amplitude.

Negatively stained specimens were made on copper grids coated with thin carbon films made by evaporation on a freshly cleaved mica surface and stripped off by flotation on water. Uranyl acetate (2% [wt/vol]) in water was used as the negative stain.

Specimens were examined in a JEOL JEM 1200 EX electron microscope fitted with a eucentric single-axis tilt specimen holder. Micrographs were recorded at 80 or 100 kV and a magnification of 60,000× with Kodak SO163 film. Tilt series were recorded at 10° intervals from +60° to −60° and were preceded and followed by zero-tilt micrographs to make sure that no degradation of the image occurred during this procedure.

Image processing. Areas of the micrographs were selected by optical diffractometry to check for coherent diffraction spots and a suitable defocus level (6) and were masked off for densitometry. The areas were then digitized with a microdensitometer constructed in this laboratory, and linked to a DEC PDP 11/60 minicomputer, which was used for all subsequent data processing. The scanning raster was set to 32 μm, which corresponds to 0.53 nm at the specimen, and areas of 256 by 256 points or 384 by 384 points were scanned.

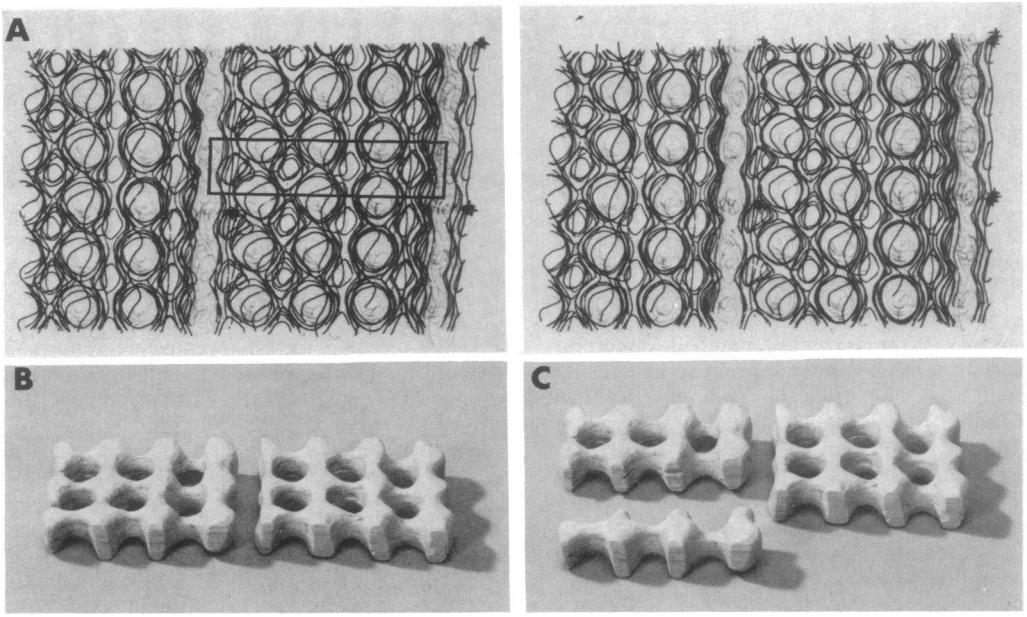

FIG. 3. Three-dimensional reconstruction of the cell sheath. (A) Stereo pair of the stack of contoured sections through the map. A unit cell is outlined. (B) Wooden model of six unit cells in the cell sheath reconstruction. (C) Wooden model like that shown in panel B but with one string of subunits displaced.

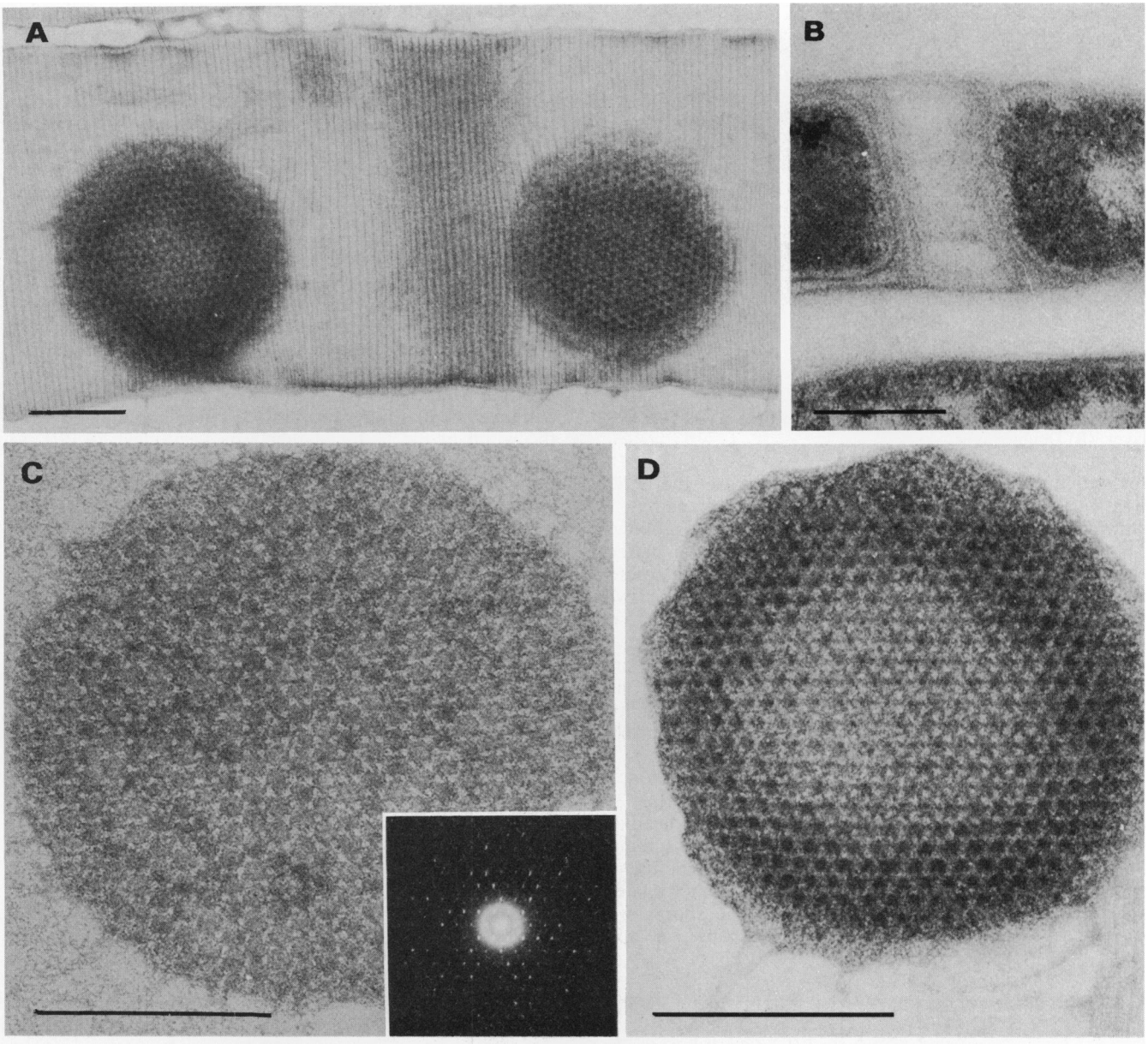

FIG. 4. Cell septa of *M. hungatei*. Bar in each photograph, 200 nm. (A) Two septa inside an intact cell sheath. (B) Section of a whole cell showing periodicities in the septa. (C) Single septum. The inset is an optical diffraction pattern of a septum. (D) Typical double-layer structure usually observed in the septa.

Processing of the images in two dimensions were carried out as described previously (14, 16). Tilt angles and axes were determined with the calculation described by Shaw and Hills (15), and the relative origins of the various data sets were determined with the phase search procedure described by Unwin and Henderson (20). In the refinement, only points on each z* line closer than 0.025 nm^{-1} were used. Amplitudes were scaled with an unweighted least-squares scale factor: $k = \Sigma F_1F_2/\Sigma F_2F_2$, summed over all points closer than 0.025 nm^{-1}. For the cell sheaths, no symmetry was present, whereas for the septa, P6 symmetry was assumed and incorporated into the origin refinement.

Regularly spaced values along the z* lines were interpolated by constrained least-squares fit with sinc functions (4) with second-derivative smoothing (11; P. J. Shaw, Ultramicroscopy, in press). The interpolated data were used as input to a three-dimensional Fourier transform program, and the reconstructed three-dimensional map was contoured with equally spaced levels in sections of constant z and traced onto transparent sheets.

RESULTS

Structure of the cell sheath. Mickle disintegration produced mainly intact sheath tubes together with some sheaths which had broken open. Typical areas, negatively stained with uranyl acetate, are shown in Fig. 1. A regular substructure was immediately visible as bands separated by fairly sharp lines of stain running laterally around the sheaths. In the intact sheaths, flattening produced back-to-back double layers. The bands of structural units could be traced around the sheath and were thus cylindrically rather than helically arranged. Single layers from broken sheaths were sought out

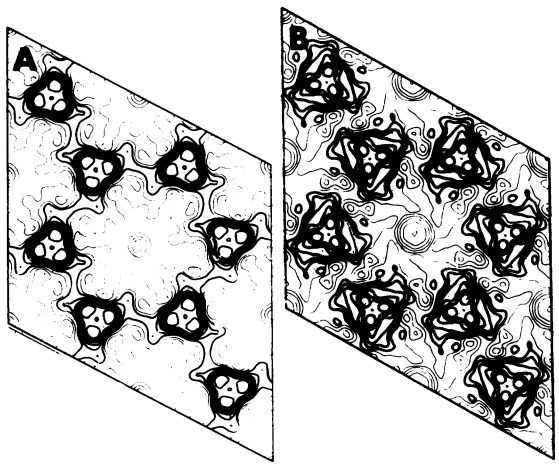

FIG. 5. Two-dimensional reconstruction of the septa. (A) Single layer. (B) Double layer.

for structural determinations. In suitable areas, the lattice was very well ordered. An optical diffraction pattern is shown in Fig. 1B. The unit cell dimensions were as follows: a = 12.0 nm, b = 2.9 nm, γ = 93.7°. The diffraction pattern showed no more than Friedel symmetry, and reconstructed zero-tilt images were not twofold symmetrical. The two-sided plane symmetry group was therefore P1 (8). The best-ordered areas showed spots extending to coordinates 8, 0 and 0, 2, corresponding to resolutions of 1.50 and 1.45 nm, respectively. For the three-dimensional reconstruction, images were included from five tilt series comprising five nontilted views and 30 tilted views up to tilt angles of 60°. Figure 2 shows a selection of z* lines.

The three-dimensional reconstruction is shown in Fig. 3. The structured layer was very thin, being no more than 3.0 to 4.0 nm in depth. The unit cell contained four beadlike subunits arranged in a straight line. These strings of subunits then packed laterally to produce the banded structure so apparent in Fig. 1. Three of the subunits were approximately spherical and 2.5 nm in diameter, and the fourth was somewhat smaller and more ellipsoidal in shape. The contacts between the fourth subunit of one string and the first subunit of the next string appeared to be very tenuous, although specific interactions must evidently exist to yield such a coherent crystal structure. Thus, the subunit associations seemed very strong within the strings of four in the repeating unit and laterally between adjacent strings, but the resulting repeating bands of structure seemed to be distinctly separate from one another. The pores through the structure were no more than 2.0 nm in diameter, and the layer is therefore probably a very effective barrier against most, if not all, proteins.

Structure of the cell septa. In negatively stained cell wall specimens, circular, flat plates with a hexagonal crystal structure were frequently observed (Fig. 4A). We believe these plates to be the cell partitions or septa seen in sectioned cells. They were apparent inside the flattened cell sheaths as well as emerging from the sheaths and completely separate from them. When the plates were found inside the flattened sheaths, the ratio between the plate diameter and the width of the flattened tube was very close to 2/Π, as would be required for circular partitions in the cylindrical tubes. A regular substructure in the septa was sometimes observed in micrographs of sectioned spirilla (Fig. 4B).

The plates were usually almost perfectly circular and were remarkably uniform in size, having a diameter of just over 0.4 μm. They generally had the appearance shown in Fig. 4D. However, the observation of occasional images like that shown in Fig. 4C means that the image in Fig. 4D represents at least a double layer. This was confirmed by the appearance of the plates on tilting. An optical diffraction pattern (inset in Fig. 4C) showed spots to ca. 2.0 nm. Two-dimensional reconstructions of the single- and double-layer plates are shown in Fig. 5A and B, respectively. Both showed P6 symmetry, indicating that the two layers have the same polarity (front to back rather than back to back). The unit cell dimensions were a = b = 18.2 nm.

For the three-dimensional reconstruction, 3 nontilted and 12 tilted images of single layers were combined, assuming P6 symmetry. Some of the z* lines are shown in Fig. 6. A stack of contoured sections through the three-dimensional reconstruction and a wooden model of a single layer are shown in Fig. 7. The single layer was 4 to 5 nm in thickness.

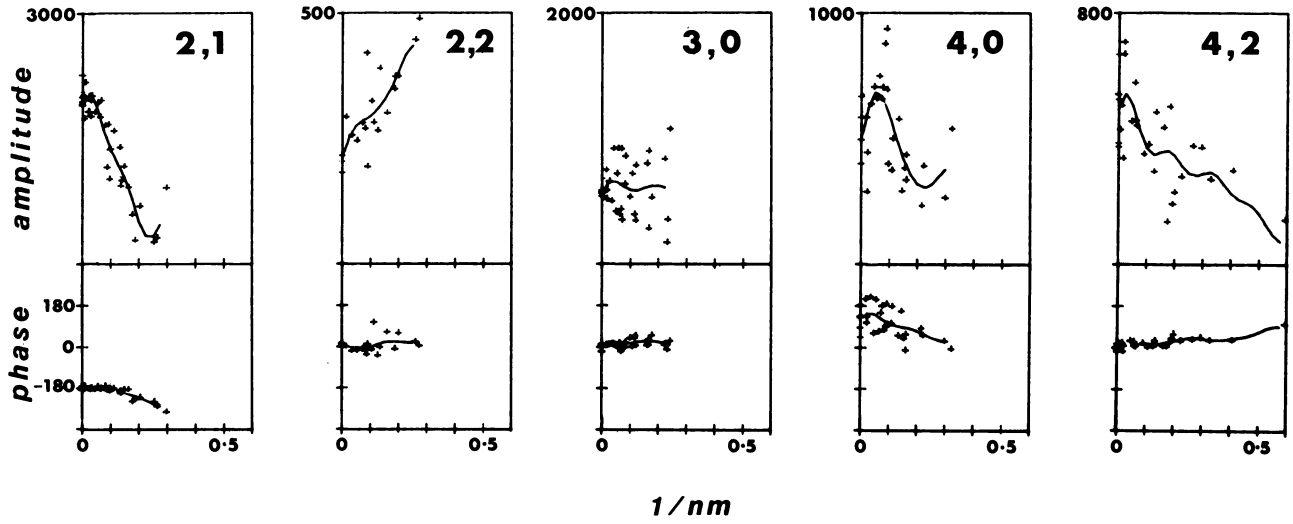

FIG. 6. Selection of z* lattice lines for the septa shown as described in the legend to Fig. 2. Phase antisymmetry was not included in the fitting.

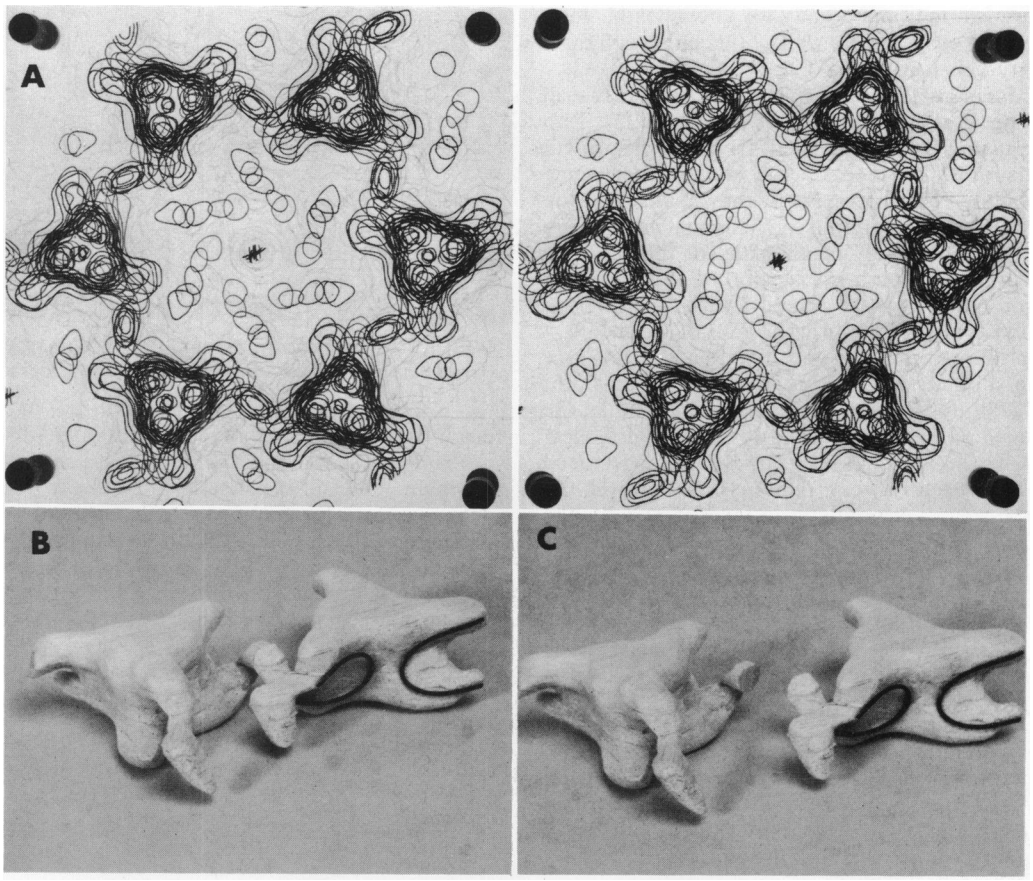

FIG. 7. Three-dimensional reconstruction of the cell septa. (A) Stereo pair of the stack of contoured sections through the map. (B) Wooden model of part of the reconstruction, showing two trimeric units (i.e., six identical subunits). The lines on two of the subunits on one of the trimers were added to clarify the subunit shape, which extends from the region of contact with the adjacent trimer up through the body of the trimer and out into a trailing tail, thus forming a hairpin structure. (C) Wooden model like that shown in panel B but with one trimer displaced so as to show the trimer-trimer interface more clearly.

Interpretation of the structure is, as in the case of the cell sheath, quite easy. The predominant feature was of subunits forming what are evidently quite close associations to produce trimers. The subunits also interacted across dimer axes, thus linking the trimers together in an open hexagonal mesh which contained holes of only one crystallographic type with a diameter of ca. 15 nm. The subunits had a "hairpin" structure, extending from the dimer axis up through the main body of the trimer and out into a trailing tail. There were indications of this tail extending into the pore towards the hexad axis. This tail extension seemed more pronounced in the double-layer two-dimensional reconstruction (cf. Fig. 5A and B). In the normal double-layer plate, the two single layers packed exactly on top of one another.

DISCUSSION

In common with other investigators (19), we have been unable to dissociate the cell sheath into its component subunits and thus have no independent evidence for their relative molecular mass. We cannot therefore say unequivocally whether the beadlike domains in the structure are discrete protein subunits or whether they are domains within a single polypeptide chain. However, we frequently saw crystal imperfections in which a band contained three or five subunits in each string rather than four subunits (Fig. 8). This suggests that the strings are put together from individual subunits at some stage and that each subunit represents at least one separate polypeptide chain. The fact that the shorter or longer strings extend in bands around the sheath indicates that individual units are probably added at the time of their incorporation into the sheath rather than that they are preformed into strings. It is entirely possible that the subunits are covalently cross-linked after being incorporated into the sheath, and this would explain our inability to dissociate the sheath into subunits. The contact between the last subunit of one string and the first subunit of the next string is obviously the weakest point of the structure and is where the structure breaks laterally as it presumably must at some stage during the life cycle of this organism.

We have not observed any square end plates such as those described by Zeikus and Bowen (22). The usual architecture at the end of a tube consisted of a single septum with a small length of sheath extending beyond it (Fig. 9A). This is what would be expected when a filament breaks in two in the region between the two septa between adjacent cells in the filament. Quite often one end was rounded beyond the terminal septum. When flattened onto the grid during negative staining, the opening at the end of the sheath can be folded into a parallelogram (Fig. 9B). We believe that this is the origin of the square end components previously reported. The rounded region of the sheath had the same

crystal structure as the main body of the sheath. It is possible that it is a vestige of the wall of the single cell from which the colony developed.

Cell division occurs within the outer sheath, the inner wall layer invaginating as the daughter cells separate (22). Two new pairs of septa must then be formed. Division and growth within the constraint provided by the sheath pose some interesting problems. The diameters of the sheaths and the septa are remarkably constant, and the filaments grown only by elongation. The most likely mechanism for the concomitant growth of the cell sheath is insertion of new bands of subunits into the middle of the crystal lattice; the alternative—the addition of new subunits at the ends of the sheath—would create problems in the control of the synthesis or transport of the subunits to the ends of the sheath or both. Although this is not impossible, it seems less likely than the former mechanism. The obvious sites for insertion of new subunits would be the gaps between the bands, and indeed because of the apparently very tight associations of the subunits it would seem very difficult to insert new subunits anywhere else in the structure. Because the unit cell angle is slightly greater than 90°, successive bands are slightly rotated with respect to one another, and the whole sheath is thus in fact a helix. The introduction of new bands into the middle of the sheath means that the helical twist must be increased. This may set up stresses which could cause the helical supercoil configuration that the filaments adopt.

Forming a closed surface from a plane lattice presents a problem for any organism adopting this form of outer cell wall layer, similar to the problems elucidated by Caspar and Klug (3) for viral capsids. A plane lattice can only be formed into the topological equivalent of a sphere by the inclusion of wedge disclinations whose algebraic angular sum is 4Π (7, 10). The cell wall of *Sulfolobus* spp. and presumably most other hexagonal surface layers contain a minimum of 12

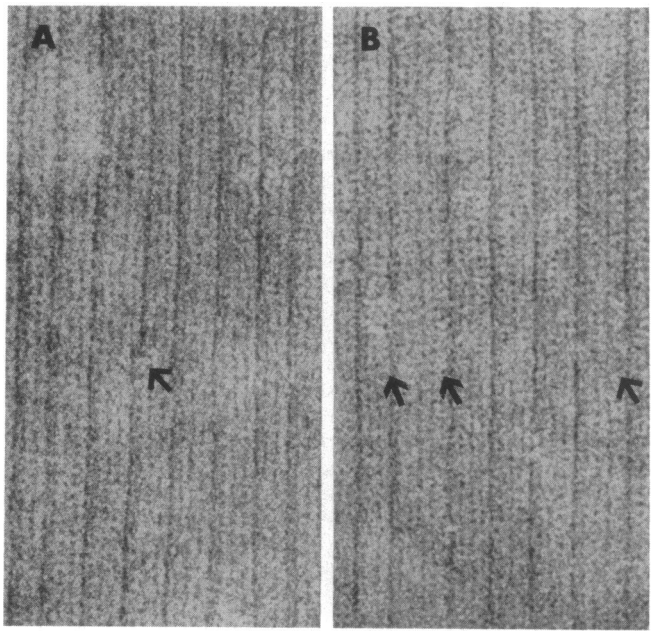

FIG. 8. Defects observed in the cell sheath crystals. (A) In the region indicated by the arrow, two bands of four subunits each become a band of three subunits and a band of five subunits. (B) Area containing a band of three subunits and two bands of five subunits each (indicated by arrows).

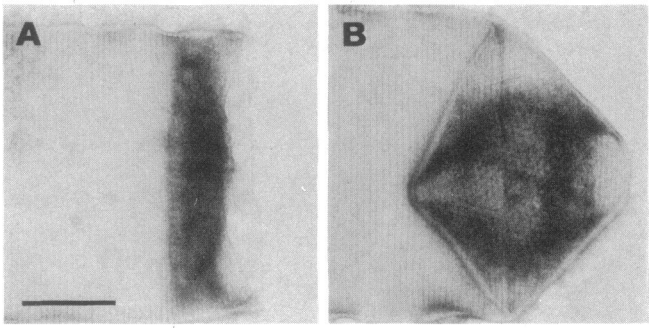

FIG. 9. Sheath ends with septa. Bar, 200 nm. (A) Edge-on view. (B) Collapsed sheath folding to form a parallelogram.

disclinations of angle Π/3 (5). Although disclinations are probably present in the rounded sheath ends of *M. hungatei*, the main bodies of the sheaths are entirely free of this lattice defect (except for the wedge disclination of 2Π which any cylinder possesses). Rather than forming a single type of crystal lattice into a closed surface, this organism has adopted the unusual strategy of producing a cylindrical surface and closing off the ends with flat disks of a different crystalline composition.

ACKNOWLEDGMENT

We thank K. Plaskitt for preparing the thin sections.

LITERATURE CITED

1. **Archer, D. B., and N. R. King.** 1983. A novel ultrastructural feature of a gas-vacuolated *Methanosarcina*. FEMS Microbiol. Lett. **16**:217–223.
2. **Balch, W. E., G. E. Fox, L. J. Magnum, C. R. Woese, and R. S. Wolfe.** 1979. Methanogens: reevaluation of a unique biological group. Microbiol. Rev. **43**:260–296.
3. **Caspar, D. L. D., and A. Klug.** 1962. Physical principles in the construction of regular viruses. Cold Spring Harbor Symp. Quant. Biol. **27**:1–24.
4. **Crowther, R. A., D. J. de Rosier, and A. Klug.** 1970. The reconstruction of a three-dimensional structure from projections and its application to electron microscopy. Proc. R. Soc. London Ser. A **317**:319–340.
5. **Deatherage, J. F., K. A. Taylor, and L. A. Amos.** 1983. Three dimensional arrangement of the cell wall protein of *Sulfolobus acidocaldarius*. J. Mol. Biol. **167**:823–852.
6. **Erickson, H. P., and A. Klug.** 1971. Measurement and compensation of defocussing and aberrations by Fourier processing of electron micrographs. Philos. Trans. R. Soc. London Ser. B **261**:105–118.
7. **Harris, W. F.** 1974. The geometry of disclinations in crystals, p. 57–93. *In* M. W. Roberts and J. M. Thomas (ed.), Surface and defect properties of solids, vol. 3. American Chemical Society, Washington, D.C.
8. **Holser, W. T.** 1958. Point groups and plane groups in a two-sided plane and their sub-groups. Z. Kristallogr. Kristallgeom. Krystallphys. Krystallchem. **110**:266–281.
9. **Hungate, R. E.** 1969. A roll tube method for cultivation of strict anaerobes, p. 117–132. *In* J. R. Norris and D. N. Ribbons (ed.), Methods in microbiology, vol. 3B. Academic Press, Inc., New York.
10. **Nabarro, F. R. N., and W. F. Harris.** 1971. Presence and function of disclinations in surface coats of unicellular organisms. Nature (London) **232**:423.
11. **Phillips, D. L.** 1962. A technique for the numerical solution of certain integral equations of the first kind. J. Assoc. Comput. Mach. **9**:84–97.
12. **Roberts, K.** 1974. Crystalline glycoprotein cell walls of algae: their structure, composition and assembly. Phil. Trans. R. Soc.

London Ser. B **268**:129–146.
13. **Roberts, K., G. J. Hills, and P. J. Shaw.** 1982. The structure of algal cell walls, p. 1–40. *In* J. R. Harris (ed.), Electron microscopy of protein, vol. 3. Academic Press, Inc., New York.
14. **Roberts, K., P. J. Shaw, and G. J. Hills.** 1981. High resolution electron microscopy of glycoproteins: the crystalline cell wall of *Lobomonas*. J. Cell Sci. **51**:295–313.
15. **Shaw, P. J., and G. J. Hills.** 1981. Tilted specimens in the electron microscope: a simple specimen holder and the calculation of tilt angles for crystalline specimens. Micron **12**:279–282.
16. **Shaw, P. J., and G. J. Hills.** 1982. Three-dimensional structure of a plant cell wall glycoprotein. J. Mol. Biol. **162**:459–471.
17. **Sleytr, U. B., and P. Messner.** 1983. Crystalline surface layers on bacteria. Annu. Rev. Microbiol. **37**:311–339.
18. **Sprott, G. D., J. R. Colvin, and R. C. McKellar.** 1979. Spheroplasts of *Methanospirillum hungatii* formed upon treatment with dithiothreitol. Can. J. Microbiol. **25**:730–738.
19. **Sprott, G. D., and R. C. McKellar.** 1979. Composition and properties of the cell wall of *Methanospirillum hungatii*. Can. J. Microbiol. **26**:115–120.
20. **Unwin, P. N. T., and R. Henderson.** 1975. Molecular structure determination by electron microscopy of unstained crystalline specimens. J. Mol. Biol. **94**:425–440.
21. **Woese, C. R., and G. E. Fox.** 1977. Phylogenetic structure of the procaryotic domain: the primary kingdoms. Proc. Natl. Acad. Sci. U.S.A. **74**:5088–5090.
22. **Zeikus, J. G., and V. G. Bowen.** 1975. Fine structure of *Methanospirillum hungatii*. J. Bacteriol. **121**:373–380.